Microscopic origin of compressive strain in hydrogen-irradiated dilute GaAs_{1−y}N_{y} alloys: Role of N-H_{n} centers with n>2 and their thermal stability

L. Wen, M. Stavola, W. B. Fowler, R. Trotta, A. Polimeni, M. Capizzi, G. Bisognin, M. Berti, S. Rubini, and F. Martelli

Phys. Rev. B **86**, 085206 — Published 22 August 2012

DOI: 10.1103/PhysRevB.86.085206

Microscopic origin of *compressive* strain in hydrogen-irradiated dilute $GaAs_{1-y}N_y$ alloys: role of $N\text{-}H_n$ centers with n>2 and their thermal stability

L. Wen,[1] M. Stavola,[1,*] W. B. Fowler,[1] R. Trotta,[2] A. Polimeni,[2] M. Capizzi,[2] G. Bisognin, [3] M. Berti,[3] S. Rubini,[4] F. Martelli[4]

[1]Department of Physics and Sherman Fairchild Laboratory, Lehigh University, Bethlehem, Pennsylvania 18015

[2]CNISM and Dipartimento di Fisica, Sapienza Universitá di Roma, I-00185 Roma, Italy

[3]MATIS CNR-INFM and Dipartimento di Fisica, Università di Padova, via Marzolo 8, 35131

[4]TASC Laboratory, IOM-CNR Strada Statale 14, Km. 163.5, I-34149 Trieste, Italy

Abstract

The addition of a few percent nitrogen to GaAs causes a large reduction of the band-gap energy and a tensile strain within the lattice. The further addition of H at 300 °C causes a recovery of the band gap of the N-free GaAs host. Concomitantly, tensile strain turns into compressive strain. Upon reduction of hydrogenation temperature, high-resolution X-ray diffraction studies show now a remarkable increase of compressive strain, while photoluminescence measurements show that the recovered band gap energy of GaAs does not change. IR measurements indicate that several $N\text{-}H_n$ centers are formed in addition to the well established H-N-H center (n=2), which accounts for the band gap recovery. The vibrational properties of the corresponding deuterium centers provide clues to the microscopic structures of these centers. Furthermore, theory shows that the center with n=2 is robust when additional H is added in its vicinity and remains as a core of likely $N\text{-}H_n$ defects.

I. Introduction: N-H_n centers in dilute III-N-V alloys

The addition of a few percent N to GaAs to form a dilute $GaAs_{1-y}N_y$ alloy causes a large reduction of the GaAs band gap.[1-4] The further addition of H (or D) to $GaAs_{1-y}N_y$ (at a temperature of 300°C to increase H diffusion) eliminates the reduction of the band gap caused by N.[5-8] Vibrational spectroscopy finds a defect with two inequivalent N-H (or N-D) stretching modes with frequencies of 3195 (2376) and 2967 (2217) cm^{-1} (Fig.1).[9] The *partial* substitution of H by D shows that the two N-H (or N-D) vibrational modes are weakly coupled.

Theory has shown that a D-N-D complex in $GaAs_{1-y}N_y$ (inset to Fig. 1) eliminates the band gap shift caused by N and explains the experimentally observed vibrational properties of the deuterated alloy.[10-13] (The deuterated D-N-D defect is more easily studied by vibrational spectroscopy than the corresponding H-N-H center and is the focus of the present paper.) The results of x-ray absorption near-edge spectroscopy (XANES) experiments and their interpretation have also been found to be consistent with a D-N-D complex.[12]

The perturbation of the vibrational properties of $GaAs_{1-y}N_y$:D by uniaxial stress has provided an elegant strategy to determine experimentally, from the stress-induced splitting and dichroism of the infrared (IR) lines,[14,15] the detailed microscopic properties of the D-N-D center that gives rise to the band gap shift.[16] From a study of the stress-induced splitting of the 2217 cm^{-1} line, the symmetry of the defect was found to be C_{1h} and the cant angle θ was determined (inset to Fig. 1). From the stress-induced dichroism that was produced and its annealing behavior, the energy lowering produced by the canting distortion[11,16] was determined.

The small N atom substituting for As in the GaAs lattice creates a tensile strain. When D is added at 300 °C, the tensile strain is converted into a compressive strain (i.e. the lattice constant of $GaAs_{1-y}N_y$:D is

larger than that of GaAs), as shown by careful high-resolution x-ray diffraction (HRXRD) measurements.[7,8,17-19] In a study by Berti *et al.,* x-ray rocking curves were measured for a $GaAs_{0.9878}N_{0.0122}$ sample that had been deuterated at 300 °C and then subsequently annealed at different temperatures.[18,19] Following a long anneal (16 h) at 250 °C, the overall strain of deuterated $GaAs_{1-y}N_y$ was reduced to zero while the band gap shift caused by deuteration remained unchanged, as shown by photoluminescence measurements. Subsequent annealing at still higher temperature (328 °C for 4h) eventually eliminated the band gap shift caused by D and recovered the tensile strain that is characteristic of the $GaAs_{1-y}N_y$ alloy without D (or H). These results show that multiple defects form upon sample deuteration, with different dissociation energies: One defect, with higher dissociation energy (1.89 eV), causes a shift of the band gap and eliminates the tensile strain in the $GaAs_{1-y}N_y$ layer, while additional defects, with lower dissociation energies (~1.77 eV), give rise to a strong compressive strain while maintaining the shift of the band gap.[18,19]

Samples that had been fully deuterated to produce a compressive strain were further studied by a suite of complementary methods: nuclear-reaction analysis, HRXRD, Rutherford backscattering, and photoluminescence.[18,19] These experiments have suggested that 3 deuterium atoms can be trapped in the vicinity of N to eliminate the band gap shift caused by N and also create a compressive strain. Theory has suggested possible defect structures in which one or two additional D atoms can be bound to the Ga atoms in the D-N-D structure that is shown in Fig. 1 to produce a modified D-N-D center.[20,21] HRXRD and XANES experiments performed on deuterated samples where a compressive strain was present are also consistent with a D-N-D structure that is modified by the further addition of nearby D atoms.[17-19,22]

In the present paper, IR spectroscopy of deuterated $GaAs_{1-y}N_y$ provides evidence of $N\text{-}D_n$ complexes with $n\geq2$, with populations depending on deuteration temperature, while complementary theory probes the microscopic structures and properties of these complexes. We note that deuteration at reduced

temperatures is of particular interest because it has been found to give rise to sharp indiffusion profiles, a result that has been exploited to fabricate novel, band-gap-engineered nanostructures.[23-25]

II. Experimental and theoretical procedures

A. Experiment

$GaAs_{1-y}N_y$ epitaxial layers were grown for our experiments by plasma-assisted, solid-source MBE on undoped, (001)-GaAs substrates. A 230 nm thick layer of $GaAs_{0.987}N_{0.013}$ was grown on a 0.5 mm thick GaAs substrate for complementary HRXRD and IR absorption measurements. For thermal annealing experiments, a 350 nm thick $GaAs_{0.9913}N_{0.0087}$ layer was grown on a GaAs substrate that was 2 mm thick.

Hydrogenation or deuteration of samples was performed with a Kaufman ion source with samples held at fixed temperatures between 200 and 300 °C. The ion energy was 100 eV, and current densities of ~10 $\mu A/cm^2$ were used. Photoluminescence measurements were performed following treatment to confirm the band gap shifts caused by H or D.

IR absorption spectra were measured with a Bomem DA.3 Fourier transform spectrometer equipped with a KBr beamsplitter and an InSb detector. The IR frequency range near 2250 cm^{-1}, where the D-stretching modes occur, yields spectra with a substantially greater signal-to-noise ratio than the frequency range where the corresponding H modes occur; therefore, we have chosen to focus on the D-N-D based complexes.

B. Theory

Theoretical calculations were performed as extensions of those reported in ref. 10 and were carried out with the CRYSTAL2006 code[26] using DFT with a gradient-corrected approximation to the exchange-correlation functional (Becke's B3LYP potential[27] with 20 % exact exchange and Lee-Yang-Parr correlation[28]). The calculations were carried out in a periodic supercell with two or more hydrogen impurities and 54 host atoms, with a computed GaAs lattice constant of 5.77 Å. A 4 x 4 x 4 k-point mesh of Monkhorst-Pack[29] type was used. The SCF energy convergence criterion was 10^{-10} Ha.

Gaussian basis functions[30] were of the type s(3)s(1)s(1)p(1) for hydrogen and s(7)sp(3)sp(1)sp(1) for nitrogen. For gallium and arsenic, most of the calculations utilized Barthelet-Durand[31] pseudopotentials, with corresponding basis functions.

III. Experimental results

To investigate the microscopic structures of defects that might be responsible for the compressive strain observed in $GaAs_{1-y}N_y$ samples deuterated at reduced temperatures, a set of 230 nm thick, $GaAs_{0.987}N_{0.013}$ samples were prepared for complementary HRXRD and IR absorption measurements by deuterium treatments at different temperatures between 200 and 280 °C. The x-ray diffraction rocking curves in Fig. 2(a) show that samples deuterated with doses between 3.0 and $5.0x10^{18}$ ions/cm^2 have compressive strains with greater magnitudes for samples deuterated at lower temperatures.[32] Fig. 2(b) shows IR absorption spectra that were measured for these samples. The vibrational lines at 2217 and 2376 cm^{-1}, labeled N_1 and N_2 in Fig. 2(b), have been assigned previously to the D-N-D center.[10-12] In addition, a variety of weak lines is seen for epi-layers under compressive strain that have not been reported previously. The frequencies of these additional weak lines are listed in Table I.

In order to investigate these weak lines further in spectra with a greater signal-to-noise ratio, a $GaAs_{0.9913}N_{0.0087}$ sample was grown on a 2 mm-thick GaAs substrate to make possible IR measurements in a multiple-internal-reflection geometry [Fig. 3(a)]. Fig. 3(b) shows IR spectra measured with a MIR geometry for a sample treated at reduced temperature (220 ºC). The lowest spectrum was measured for a sample that had been deuterated with a dose of 6×10^{18} cm^{-2}. The spectrum just above was measured after the same sample had been deuterated further to have received a total D dose of 1.2×10^{19} cm^{-2}. The uppermost spectrum is the difference of the spectra measured for the high and low dose samples. The bands that are seen can be grouped into pairs, a result that will be reinforced by annealing data to be presented below.

Lines labeled C_1 and C_2 are produced with the first deuterium treatment along with the lines at 2217 and 2376 cm^{-1} labeled N_1 and N_2 assigned previously to the "bare" D-N-D center.[10-12] The addition of further D strengthens the lines A_1 and A_2 and also the broad bands labeled B_1 and B_2. The second D treatment also weakens the N_1 and N_2 lines of the "bare" D-N-D center. These results are all consistent with the formation of *perturbed* D-N-D centers whose concentrations are increased by the addition of more D at the expense of the concentration of the "bare" D-N-D center.

Fig. 4 shows annealing results for a $GaAs_{0.9913}N_{0.0087}$ MIR sample that was deuterated at 220 °C with a dose of 1.2×10^{19} cm^{-2}. Fig. 5 shows differences of spectra calculated for successive anneals to reveal the changes that occur at each stage of annealing. Upon annealing at 200 °C, bands A_1 and A_2 begin to be annealed away together. At 250 °C, the annealing of bands A_1 and A_2 is completed and the bands B_1 and B_2 are also annealed away. As the A_1, A_2, B_1, and B_2 features are annealed away at 200 and 250 °C, the N_1 and N_2 lines assigned to the "bare" D-N-D center increase in strength. These results show that the bare D-N-D structure is recovered as the perturbed D-N-D centers are annealed away.

At 300 °C, the C_1 and C_2 lines are annealed away and the N_1 and N_2 lines also begin to disappear, as shown in Fig. 4 and Fig. 5. A close look at Fig. 4 also shows that shoulders to the N_1 and N_2 lines, labeled S_1, S_2, and S_3, grow in strength beginning at 250 °C as the A, B, and C lines are annealed away. Fig. 4(b) shows an expansion of the region near the N_2 line so that the shoulder labeled S_3, and its annealing behavior, can be seen more clearly. S_3 is seen to have an annealing behavior similar to that of the S_1 and S_2 lines that appear in the same spectrum. We suggest that S_1, S_2, and S_3 are due to perturbed D-N-D centers but with a smaller frequency shift than for the A, B, and C pairs of lines. In this picture, bands S_1 and S_2, with frequencies shifted slightly from the N_1 line, would be due to two different weakly perturbed D-N-D centers. S_3, with a frequency shifted slightly from the N_2 line, would then be due to these same two centers but with a line splitting that is not resolved.

Our IR results show that a single N-D_3 center is not responsible for the behavior of $GaAs_{1-y}N_y$ deuterated at reduced temperature as was suggested previously.[18,19] On the contrary, multiple defect structures are formed, each of which gives rise to an additional pair of N-D vibrational modes, all working to increase the extent of compressive strain in deuterium-irradiated $GaAs_{1-y}N_y$. While the average behavior may be consistent with previous work that suggested a D-N-D center with an additional D atom bonded nearby,[18,19] our IR data reveal that the detailed microscopic structures are more complicated with multiple centers being formed. We turn to theory to investigate what defect structures might be possible.

IV. Theoretical results

We have used CRYSTAL06 to predict structures, relative stabilities, and vibrational frequencies for defects involving two, three, four, and six H atoms, including two defects – H-N-H and H-N-H$(GaH)_2$ –

with a neighboring interstitial H_2 molecule in two possible locations, labeled (xy) and (z), respectively. (z is the [001] direction that is perpendicular to the [110] primary symmetry axis of the H-N-H core of the defect.) Several structural predictions are shown in Fig. 6. Earlier, Amore Bonapasta *et al.*[20] had carried out similar calculations using density functional theory. Comparison of Fig. 6 with Fig. 1 of Ref. 20 shows remarkable structural agreement for the two, three, and four H defects which they considered, which is gratifying considering that the two calculations involved different approaches (plane wave vs. Gaussian basis functions) and different Hamiltonians and supercell sizes. In both cases it is clear that the canted H-N-H core is a robust constituent of all of the considered defects.

By comparing total energies for various supercell configurations, we compare relative stabilities for various configurations. Several conclusions emerge from these results, shown in Table II. First and most significant, the four-H defect [Fig. 6(c)] is more stable than the three-H defect [Fig. 6(b)], which in turn is more stable than the H-N-H defect with near or far interstitial H_2 [e.g., Fig. 6(d)]. Second, the H-N-H defect with an H_2 in an adjacent (xy) cell is slightly more stable than H-N-H with a separated H_2 (distant). However, H-N-H with H_2 in a different adjacent (z) cell (structure not shown in Fig. 6) is slightly less stable than H-N-H with a separated H_2. Similar results are obtained for the four-H defect with neighboring H_2. While all these and similar configurations are metastable, the relative energies for defects that involve H_2 in different cells are very small, of order 0.1 eV, so conclusions involving their relative stabilities are not easily established.

The vibrational properties of the defects shown in Fig. 6 are similar because they are determined by the weakly coupled N-D modes of the D-N-D unit at the core of each structure.[33] This makes it difficult to assign specific vibrational modes to a particular structure. Nonetheless, the signs and magnitudes of the frequency shifts of the N-D modes that occur when additional D atoms are added can be determined by theory to provide clues that suggest specific assignments.

Our computed harmonic vibrational frequencies have been scaled by factors which we obtained from anharmonicity calculations using CRYSTAL06 under identical conditions for an NH_2 molecule. The resulting frequencies for the H-N-H (or D-N-D) defects, 3110 (2291) and 2795 (2052) cm^{-1}, respectively, while in only fair agreement with experiment, serve as bases for comparison as more complex defects are considered. Calculated frequency shifts for selected D-N-D defects are given in Table III, along with values estimated from the H-N-H frequencies given in Table III of Ref. 20. Corresponding experimental frequency shifts from Table I are also shown. We believe that these results provide evidence that the lines B_1 and B_2 arise from the three-D defect, and also provide good support that either A_1 and A_2 or C_1 and C_2 involve the four-D defect. We suggest, furthermore, that S_1, S_2, and S_3 involve D-N-D with an adjacent D_2 molecule. Furthermore, either the A pair or the C pair may well involve the four-D defect with an adjacent D_2 molecule.

V. Conclusion

The addition of H (or D) to dilute $GaAs_{1-y}N_y$ alloys at temperatures above 300 °C produces an H-N-H (or D-N-D) complex that shifts the band gap to its N-free value and gives rise to a *compressive* strain within the lattice, that increases with N concentration.[7,8] Annealing experiments performed for deuterated $GaAs_{1-y}N_y$ samples have shown that the changes in lattice strain and band gap have different dependences on the annealing temperature, revealing that multiple defect process are responsible for these effects.[18,19]

The present investigation by vibrational spectroscopy finds several new N-D modes and an increasing compressive strain in $GaAs_{1-y}N_y$ samples deuterated at reduced temperatures. Investigations of the introduction of these lines for increasing D doses and of their annealing behaviors as a function of temperature suggest that these lines occur as pairs, labeled as A, B, and C, with slightly different thermal stabilities.

For all of our annealing experiments, we find that there is common behavior. As the A, B, and C line pairs are annealed away, the N-D lines of the bare D-N-D center as well as the side bands to these lines (labeled S) grow in intensity. An explanation is that when additional D atoms are added to the bare D-N-D center and become bonded nearby, they shift the N-D IR lines to give rise to two new N-D modes for each different perturbed center. Upon annealing, the additional D atoms are dissociated from the D-N-D core and either the N-D lines of the bare D-N-D center recover or the perturbed lines shift closer to their unperturbed positions to give rise to shoulders to these lines.

Theory reaches similar conclusions and suggests specific defect structures (Fig. 6). Additional D (or H) is bonded to the D-N-D core at nearby Ga atoms[33] or as nearby interstitial D_2 (or H_2) molecules. The basic D-N-D structure is found to be robust by theory and persists when additional D atoms become bonded nearby.

In summary, the IR results presented here and their interpretation reveal atomic-scale information about the structures of N-D_n centers in $GaAs_{1-y}N_y$:D that contain more than two D atoms. They establish that several structures with a D-N-D core and slightly different thermal stabilities are formed, with relative concentrations depending on deuteration temperature. These results provide a detailed microscopic explanation for the results of *in situ* HRXRD studies of deuterated $GaAs_{1-y}N_y$ samples.[18,19]

VI. Acknowledgment

The research performed at L.U. was supported by NSF grants DMR-0802278 and DMR 1160756.

References

1. M. Weyers, M. Sato, and H. Ando, Jpn. J. Appl. Phys. **31**, L853 (1992).
2. W.G. Bi and C.W. Tu, Appl. Phys. Lett. **70**, 1608 (1997).
3. *Dilute Nitride Semiconductors,* edited by M. Henini, (Elsevier, Amsterdam, 2005).
4. *Physics and Applications of Dilute Nitrides,* edited by I. A. Buyanova and W. M. Chen (Taylor & Francis, New York, 2004).
5. A. Polimeni, G. Baldassarri H.v.H., M. Bissiri, M. Capizzi, M. Fischer, M. Reinhardt, and A. Forchel, Phys. Rev. B **63**, 201304(R) (2001).
6. A. Polimeni, G. Baldassarri H.v.H., M. Bissiri, M. Capizzi, A. Frova, M. Fischer, M. Reinhardt, and A. Forchel, Semicond. Sci. Tech. **17**, 797 (2002).
7. A. Polimeni, G. Ciatto, L. Ortega, F. Jiang, F. Boscherini, F. Filippone, A. Amore Bonapasta, M. Stavola, and M. Capizzi, Phys. Rev. B **68**, 85204 (2003).
8. A. Polimeni and M. Capizzi, Chapt. 6 in *Physics and Applications of Dilute Nitrides,* ref. [4].
9. F. Jiang, M. Stavola, M. Capizzi, A. Polimeni, A. Amore Bonapasta, and F. Filippone, Phys. Rev. **69**, 041309(R) (2004).
10. W. B. Fowler, K. R. Martin, K. Washer, and M. Stavola, Phys. Rev. **72**, 035208 (2005).
11. M.-H. Du, S. Limpijumnong, and S.B. Zhang, Phys. Rev. B **72**, 073202 (2005).
12. G. Ciatto, F. Boscherini, A. Amore Bonapasta, F. Filippone, A. Polimeni, and M. Capizzi, Phys. Rev. B **71**, 201301(R) (2005).
13. H.C. Alt, P. Messerer, K. Kohler, and H. Riechert, Phys. Status Solidi B **246**, 200 (2009) report IR results that led these authors to suggest that a D-N-D complex is not responsible for the IR lines at 2217 and 2376 cm^{-1}. However, experiments with mixed H and D isotopes that are critical for assigning these lines were not performed in this work.
14. M. Stavola, S.J. Pearton, J. Lopata, C.R. Abernathy, and K. Bergman, Phys. Rev. B **39**, 8051 (1989).

15. M. Stavola, Vibrational Spectroscopy of Light Element Impurities in Semiconductors, Chapt. 3 in *Identification of Defects in Semiconductors*, edited by M. Stavola, Vol. 51B in the series *Semiconductors and Semimetals* (Academic, Boston, 1998).
16. L. Wen, F. Bekisli, M. Stavola, W.B. Fowler, R. Trotta, A. Polimeni, M. Capizzi, S. Rubini, and F. Martelli, Phys. Rev. B **81**, 233201 (2010).
17. G. Bisognin, D. De Salvador, A. V. Drigo, E. Napolitani, A. Sambo, M. Berti, A. Polimeni, M. Felici, M. Capizzi. M. Güngerich, P. J. Klar, G. Bais, F. Jabeen, M. Piccin, S. Rubini, F. Martelli, and A. Franciosi, Appl. Phys. Lett. **89**, 061904 (2006).
18. M. Berti, G. Bisognin, D. De Salvador, E. Napolitani, S. Vangelista, A. Polimeni, M. Capizzi, F. Boscherini, G. Ciatto, S. Rubini, F. Martelli, and A. Franciosi, Phys. Rev. B **76**, 205323 (2007).
19. G. Bisognin, D. De Salvador, E. Napolitani, M. Berti, A. Polimeni, M. Capizzi, S. Rubini, F. Martelli, and A. Franciosi, J. Appl. Cryst. **41**, 366 (2008).
20. A. Amore-Bonapasta, F. Filippone, and G. Mattioli, Phys. Rev. Lett. **98**, 206403 (2007).
21. W.B. Fowler, M. Stavola, L. Wen, A. Polimeni, and M. Capizzi, Bull. Am. Phys. Soc. **54** (1), 2009 APS March Meeting, abstract number J21.00005 (2009).
22. G. Ciatto, F. Boscherini, A. Amore Bonapasta, F. Filippone, A. Polimeni, M. Capizzi, M. Berti, G. Bisognin, D. De Salvador, L. Floreano, F. Martelli, S. Rubini, and L. Grenouillet, Phys. Rev. B **79**, 165205 (2009).
23. M. Felici, A. Polimeni, G. Salviati, L. Lazzarini, N. Armani, F. Masia, M. Capizzi, F. Martelli, M. Lazzarino, G. Bais, M. Piccin, S. Rubini, and A. Franciosi, Adv. Mater. **18**, 1993 (2006).
24. R. Trotta, A. Polimeni, F. Martelli, G. Pettinari, M. Capizzi, L. Felisari, S. Rubini, M. Francardi, A. Gerardino, P. C. M. Christianen, and J. C. Maan, Adv. Mater. **23**, 2706 (2011).
25. R. Trotta, A. Polimeni, and M. Capizzi, Advanced Functional Materials (Feature article) **22**, 1782 (2012).

26. R. Dovesi, V. R. Saunders, C. Roetti, R. Orlando, C. M. Zicovich-Wilson, F. Pascale, B. Civalleri, K. Doll, N. M. Harrison, I. J. Bush, Ph. D'Arco, and M. Llunell, ***Crystal06 User's Manual***, University of Torino, Torino, 2006.

27. D. Becke, Phys. Rev. A **38**, 3098 (1988).

28. C. Lee, W. Yang, and R. G. Parr, Phys. Rev. B **37**, 785 (1988).

29. H. J. Monkhorst and J. D. Pack, Phys. Rev. B **13**, 5188 (1976).

30. Basis functions were obtained from the web site of M. D. Towler, http://www.tcm.phy.cam.ac.uk/~mdt26/crystal.html.

31. P. Durand and J. C. Barthelat, Theor. Chim. Acta **38**, 283 (1975); J. C. Barthelat and P. Durand, Gazz. Chim. Ital. **108**, 225 (1978).

32. The rocking curve for the sample deuterated at 200 ºC shows two compressive peaks. Presumably, this sample, treated at the lowest temperature shown here, is not deuterated homogeneously through its thickness.

33. We have performed additional experiments to search for Ga-H and Ga-D vibrational modes because D-N-D-$(Ga-D)_n$ centers are candidates for the perturbed D-N-D centers we have discovered. While spectra measured for samples hydrogenated or deuterated at 220 ºC do show broad, weak bands that might be Ga-H or Ga-D modes, these features were not seen with sufficient signal-to-noise ratio for us to make assignments with any confidence. The question of whether or not Ga-H or Ga-D bonds are formed in our samples is not answered by our IR data. L. Wen, Ph.D. dissertation, Lehigh University, Bethlehem, PA, 2010.

Table I. Frequencies, in cm^{-1}, of additional IR lines observed for $GaAs_{1-y}N_y$ epitaxial layers deuterated at temperatures between 200 and 280 °C.

B_1	S_1	S_2	A_1	C_1	S_3	B_2	C_2	A_2
2190	2224	2251	2264	2280	2379	2389	2459	2476

Table II. Relative energies of different metastable configurations of GaAs:N:H_n, computed by CRYSTAL06. NH_3 is H-N-H-(Ga-H) and NH_4 is H-N-H-$(Ga-H)_2$. The labels in parentheses refer to the labels of structures shown in Fig. 6 or defined in the text (z).

Lower	*Higher*	*energy difference (eV)*
NH_4 (c)	$NH_3 + 0.5xH_2$ distant (b)	1.22
NH_4 (c)	$NH_2 + H_2$ (xy) (d)	1.94
NH_4 (c)	$NH_2 + H_2$ distant	2.07
NH_4 (c)	$NH_2 + H_2$ (z)	2.21

Table III. Computed frequency shifts, in cm^{-1}, of the D-N-D modes with additional D atoms. Configurations are shown in Fig. 6: e. g., (b) - (a) gives the shifts of the higher and lower modes for D-N-D with and without an additional D attached to a Ga. Results from Ref. 20 are estimated by isotope-shifting, D for H, the values given for H defects in Table III of that paper.

	Present calculation		*From Ref. 20*			*Experiment*	
	higher	lower	higher	lower		higher	lower
(b) - (a)	25	-33	34	-30	B's	13	-27
(c) - (a)	44	119	18	28	A's	100	47
					C's	83	63
(d) - (a)	31	9	-----	-----	S_1, S_3	3	7
					S_2, S_3	3	34

Figure captions

FIG. 1. IR absorbance spectrum (4.2 K) measured with a resolution of 1 cm^{-1} for the N-D stretching modes of a $GaAs_{0.9913}N_{0.0087}$ sample. The sample was deuterated at 300 °C with a dose of $3x10^{18}$ impinging ions/cm^2. The inset shows the relaxed D-N-D defect in $GaAs_{1-y}N_y$. θ is the angle of the N-D bond that gives rise to the 2217 cm^{-1} line, measured with respect to the <001> axis that is perpendicular to the <110> primary symmetry axis of the C_{1h} center.

FIG. 2. (a) (004) x-ray diffraction rocking curves for 230 nm thick samples of $GaAs_{0.987}N_{0.013}$ after deuterium irradiation with doses between 3.0 and $5.0x10^{18}$ impinging ions/cm^2 at the temperatures shown. (b) IR absorbance spectra (4.2 K) measured with a resolution of 1 cm^{-1} for the N-D stretching modes of the $GaAs_{0.987}N_{0.013}$ samples whose x-ray diffraction rocking curves are shown in panel (a).

FIG. 3. (a) The multiple-internal-reflection geometry used to increase the signal-to-noise ratio of IR absorption measurements made for $GaAs_{1-y}N_y$ epitaxial layers grown on 2 mm thick GaAs substrates. (b) IR absorbance spectra measured in a MIR geometry for a $GaAs_{0.9913}N_{0.0087}$:D layer. The two lowest spectra are for the same sample after it was deuterated at 220 °C with the different doses that are indicated. The upper trace shows the difference of the spectra measured for the different D doses.

FIG. 4. (a) IR absorbance spectra (4.2 K) measured with a resolution of 1 cm^{-1} in a MIR geometry for a $GaAs_{0.9913}N_{0.0087}$:D layer that had been deuterated at 220 °C with a dose of $1.2x10^{19}$ impinging ions/cm^2. This sample was annealed sequentially at the temperatures indicated (°C) for 30 minutes. (a-p is for the as-prepared sample.) (b) An expansion of the spectra shown in (a) in the vicinity of the line at 2376 cm^{-1}.

FIG. 5. Difference spectra for selected sequential annealing steps for a $GaAs_{0.9913}N_{0.0087}$:D layer that had been deuterated at 220 °C with a dose of $1.2x10^{19}$ impinging ions/cm^2 and subsequently annealed for 30 minutes. These difference spectra reveal the changes in spectral-line intensities that occur between the particular annealing steps that are indicated for the series of sequential anneals whose results are shown in Fig. 4.

FIG. 6. Computed structures for GaAs:N:H_n. (a) H-N-H, (b) H-N-H plus one Ga-H; (c) H-N-H plus two Ga-H; (d) H-N-H plus interstitial H_2 in adjacent (xy) cell. [P. Ugliengo "MOLDRAW: A Program to Display and Manipulate Molecular and Crystal Structures", Torino (**2006**), available on the web at http:www.moldraw.unito.it; P. Ugliengo, D. Viterbo, and G. Chiari, *Z. Kristallogr*. **207**, 9 **(**1993**)**]

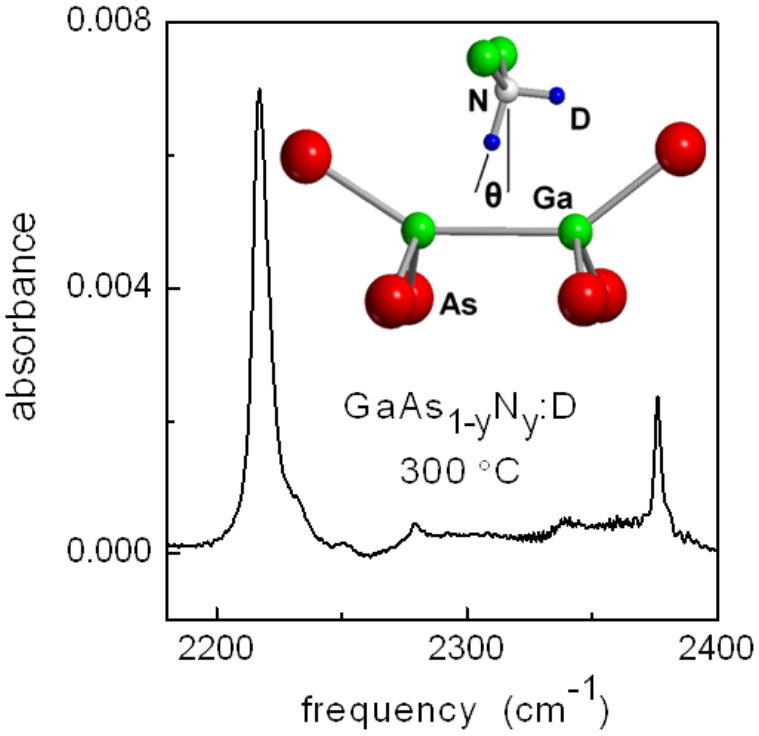
0.008
0.004
0.000
absorbance
N
D
θ
Ga
As
GaAs1-yNy:D
300 °C
2200
2300
2400
frequency (cm-1)

Fig. 1

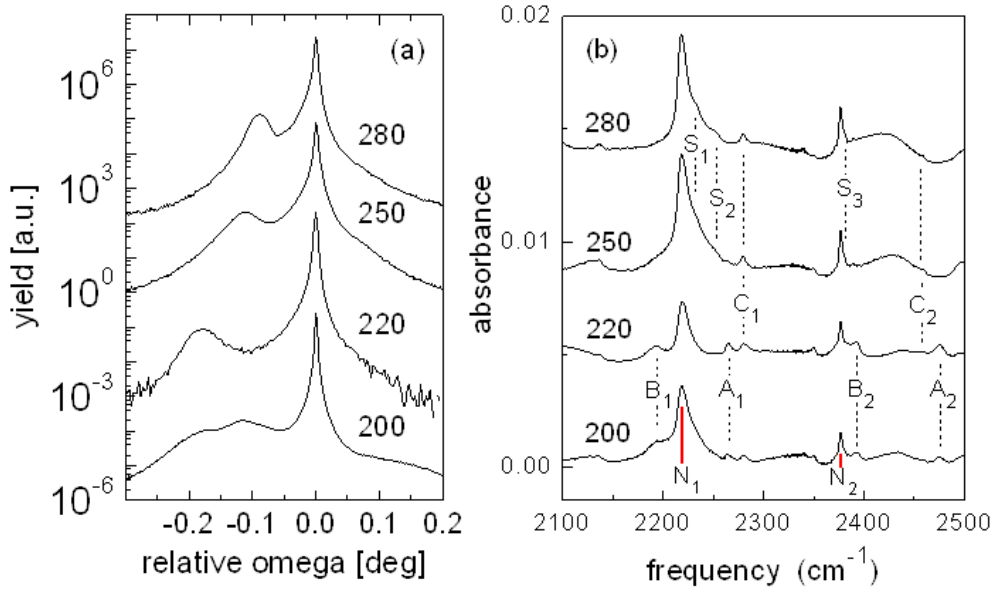
(a)
10^6
10^3
10^0
10^-3
10^-6
yield [a.u.]
280
250
220
200
-0.2 -0.1 0.0 0.1 0.2
relative omega [deg]
(b)
0.02
0.01
0.00
absorbance
S1
S2
S3
C1
C2
B1
A1
B2
A2
N1
N2
2100
2200
2300
2400
2500
frequency (cm-1)

Fig. 2

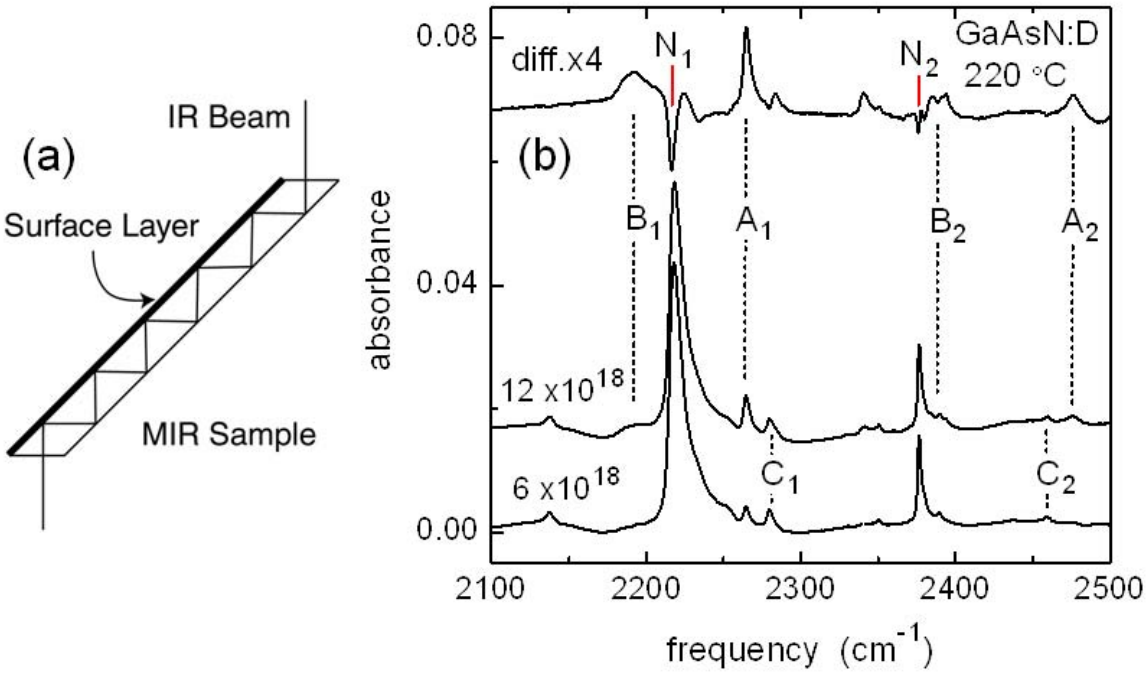
(a)
IR Beam
Surface Layer
MIR Sample
(b)
diff.x4
N1
N2
GaAsN:D
220 °C
B1
A1
B2
A2
12 x10^18
6 x10^18
C1
C2
absorbance
0.08
0.04
0.00
2100
2200
2300
2400
2500
frequency (cm^-1)

Fig. 3

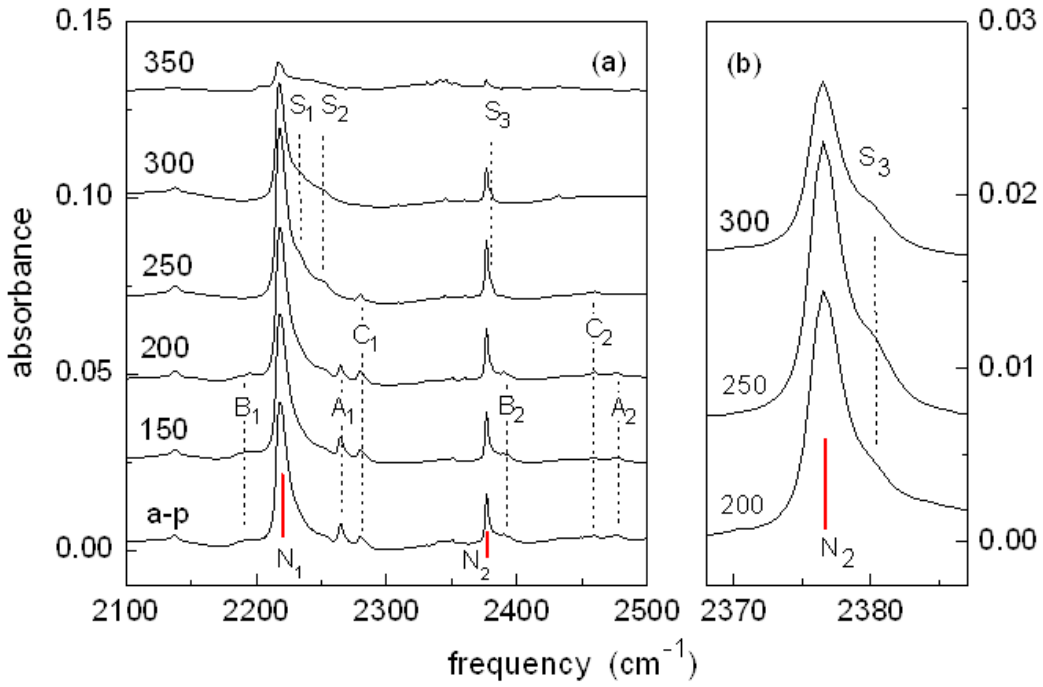
absorbance
0.15
0.10
0.05
0.00
350
300
250
200
150
a-p
(a)
S1
S2
S3
C1
C2
B1
A1
B2
A2
N1
N2
(b)
0.03
0.02
0.01
0.00
2100
2200
2300
2400
2500
2370
2380
frequency (cm^-1)

Fig. 4

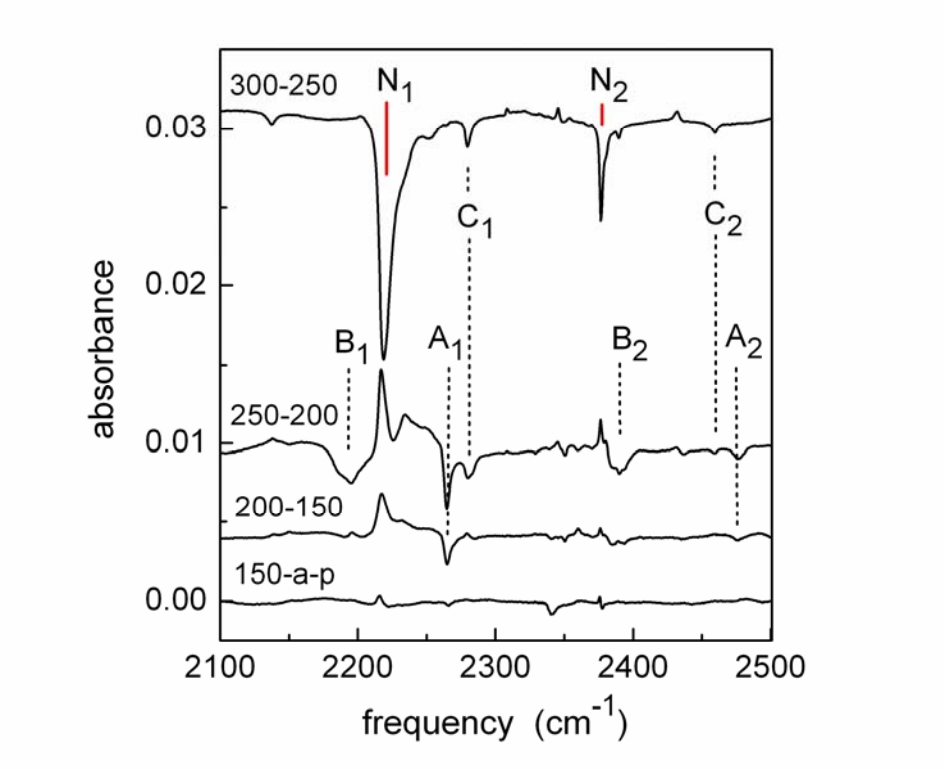
300-250
N1
N2
0.03
C1
C2
0.02
absorbance
B1
A1
B2
A2
250-200
0.01
200-150
150-a-p
0.00
2100
2200
2300
2400
2500
frequency (cm-1)

Fig. 5

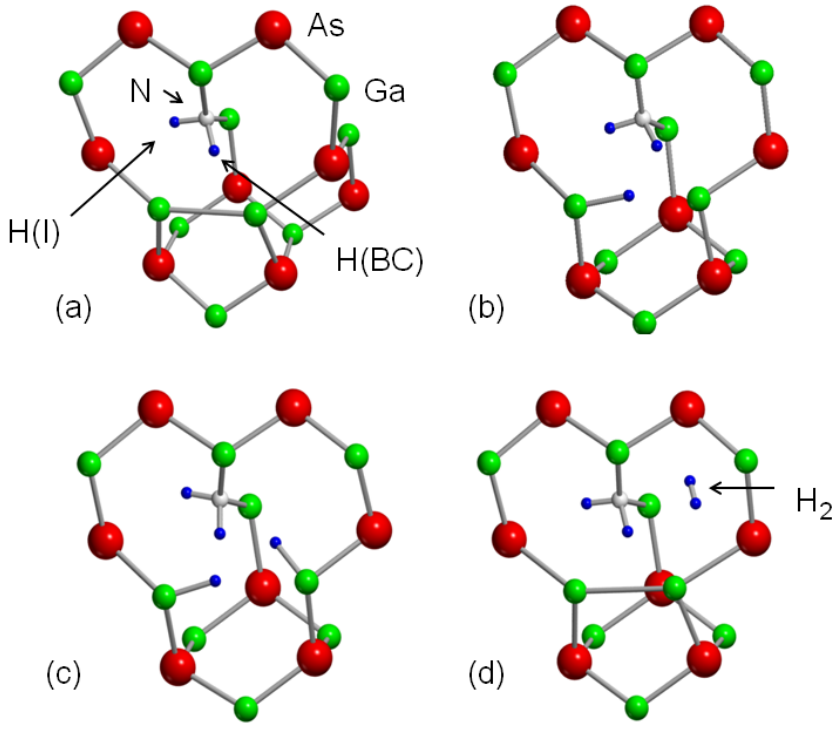
As
N
Ga
H(I)
H(BC)
(a)
(b)
(c)
(d)
H2

Fig. 6